



Synthesis, crystal structure and formation kinetics of zinc(II) and copper(II) complexes with 5,12-dimethyl-1,4,8,11-tetraazacyclotetradecane

Ki-Young Choi

Department of Chemistry, Mokwon University, Taejeon 301-729, Korea

(Received 19 August 1996; accepted 18 October 1996)

Abstract—The complex $[\text{Zn}(\text{L})\text{Cl}][\text{ClO}_4](\mathbf{1})$ (L = 5,12-dimethyl-1,4,8,11-tetraazacyclotetradecane) has been prepared and characterized by X-ray crystallography. The structure of **1** consists of isolated $[\text{Zn}(\text{L})\text{Cl}]^+$ cations and ClO_4^- counter anions. The coordination of the zinc atom is a distorted square pyramid with four nitrogens of the macrocycle occupying the basal sites [$\text{Zn}-\text{N}_{\text{av}} = 2.121(9) \text{ \AA}$] and a terminal chloride ligand at the apical position with a Zn—Cl distance of 2.275(3) Å. The complexation reactions of Zn^{2+} and Cu^{2+} with L have been studied by using stopped-flow spectrophotometry. The measurements were made at $25.0 \pm 0.1^\circ\text{C}$ in an aqueous solution of 0.10 M (NaClO_4) ionic strength. The formation reaction takes place by rapid formation of an intermediate complex ($\text{MH}_2\text{L}^{2-*}$), which proceeds to the final product in the rate-determining step. The stability constants ($\log K_{\text{MH}_2\text{L}^{2-*}}$) and specific base-catalysed rate constants (k_{OH}) of intermediate complexes have been determined from the kinetic data. In the pH range examined, the monoprotonated (HL^{3-}) form of L is the kinetically active species despite its low concentration. © 1997 Elsevier Science Ltd. All rights reserved.

Keywords: Zn^{II} and Cu^{II} complexes of tetraaza macrocycle.

Macrocyclic polyamine complexes of bivalent transition metals have been of great interest due to their importance as an essential metalloenzyme active site [1,2], and many of which are involved in bioenergetic processes. Cyclam (1,4,8,11-tetraazacyclotetradecane) is well recognized as an example among the macrocyclic polyamines in its ability to impart thermodynamic and kinetic stability to a variety of oxidation states of metal ions [3,4]. Recently, it has been reported that the modified cyclam complexes show considerable changes in physical and chemical properties, structures and catalytic efficiency [5–8]. The coordination environments around zinc ions in those complexes are known to be square pyramidal or octahedral with bonds to water [9–11] or thiocyanate [12] ligands. We also reported the crystal structure of $[\text{Cu}(\text{DTAD})(\text{SCH}_3)_3] \cdot 2\text{H}_2\text{O}$ [13] (DTAD = 3,14-dimethyl-2,6,13,17-tetraazatricyclo[14,4,0^{1,8},0^{7,12}]dicosane), in which the copper(II) ion adopts a tetra-

gonally elongated octahedral geometry with two apical thiolate sulfur atoms.

Kodama and Kimura [14,15] have carried out a series of kinetic studies of a number of transition metal ions reacting with cyclam as well as macrocycles with different ring sizes and number of nitrogen donor atoms. The attachment of potentially coordinating groups on the nitrogens of cyclam enhances the ligation possibilities of the ring. We have recently studied the kinetics for the formation of metal ion complexes with various macrocyclic ligands [16–19]. The kinetic data conformed to the rapid formation of an intermediate, which converted to the final complex, in that case the reactants interacted separately by a second-order process to give the final complex.

We report herein the synthesis and crystal structure of a zinc complex of 5,12-dimethyl-1,4,8,11-tetraazacyclotetradecane (L). We also investigated the systematic formation kinetics of Zn^{2+} and Cu^{2+}

complexes of L and the results are compared with published data on the metal complexation of cyclam.

EXPERIMENTAL

Materials

The ligand L was prepared according to previously published procedures [20]. MS (EI) Calc.(found) m/z : 228 (228) (M)⁺ Calc.(found) for $C_{12}H_{28}N_4$: C, 63.1 (63.2); H, 12.4 (12.3); N, 24.5 (24.5)%. All other chemicals were reagent grade and were used without further purification.

Synthesis of $[Zn(L)Cl][ClO_4](1)$

To a methanol solution (20 cm³) of $ZnCl_2$ (136 mg, 1 mmol) was added L (228 mg, 1 mmol) and then the mixture was heated at reflux for 2 h. Excess $NaClO_4$ was added to the solution and then the solution was placed in a refrigerator to complete the crystallization. The colorless crystals were filtered off, washed with diethyl ether and dried *in vacuo*. The product was recrystallized from water/acetonitrile (1 : 1) mixture. Yield: 309 mg (72% based on L). Calc.(found) for $ZnC_{12}H_{28}N_4O_4Cl_2$: C, 33.6 (33.8); H, 6.4 (6.4); N, 13.1 (13.0)%. FAB MS: m/z 329.22 ($M-ClO_4$)⁺.

Solution preparations

Stock solutions of Zn^{2+} and Cu^{2+} were prepared from $Zn(ClO_4)_2 \cdot 6H_2O$ and $Cu(ClO_4)_2 \cdot 6H_2O$ (Aldrich, 99.9%) and their concentrations were determined by EDTA titration using Murexide as an indicator. The concentration of a ligand stock solution was determined by titration against a standardized $Cu(ClO_4)_2$ solution using Murexide as an indicator. Sodium perchlorate (Aldrich) was used to control the ionic strength in all kinetic studies. All solution were made in deionized water.

Measurements

The study on the formation of $Zn(L)^{2-}$ was performed in weakly buffered solutions by monitoring the pH decrease (0.10–0.24 pH unit) with bromocresol green (4.58 < pH < 5.50, 615 nm) as an indicator [21]. The reaction of Cu^{2+} with L was investigated by observing the formation of complex directly at 290 nm. The concentration of the indicator was kept constant at 2.0×10^{-5} M, while that of acetate buffer varied between 5.0×10^{-3} and 2.0×10^{-2} M, independent of the reaction rate. The concentration of L was 2.0×10^{-4} M, while that of Zn^{2+} and Cu^{2+} ions was varied between 6.0×10^{-4} and 8.0×10^{-3} M.

Solution pH values were measured with a Beckman combination electrode and Beckman Model Φ 71 pH meter. The H^+ ion concentration was established from

the measured pH value in acetate buffer solution of 0.10 M ($NaClO_4$) ionic strength by the procedures reported previously [22]. All kinetic measurements were made with the use of a Hi-Tech stopped-flow spectrophotometer interfaced with a Scientific data acquisition system at $25.0 \pm 0.1^\circ C$ with the use of a Lauda RM circulatory water bath.

X-ray crystallography

All measurements were carried out on an Enraf-Nonius CAD 4 diffractometer by using the graphite-monochromated $Mo-K_\alpha$ ($\lambda = 0.71069 \text{ \AA}$) radiation and $\omega/2\theta$ scan mode at 293 K. A colorless crystal of 1 with approximate dimensions $0.30 \times 0.50 \times 0.25$ mm was mounted on the diffractometer and used for data collection. The crystal was coated with lacquer because of radiation sensitivity. The unit cell parameters and orientation matrix were obtained by the least squares fit of 25 reflections in the 2θ range 22.70 – 27.91° . Crystallographic data and refinement details are summarized in Table 1. The intensity data of the compound were reduced using Lorentz and polarization corrections but no absorption correction was applied. After the reduction step all calculations were performed using the NRCVAX PC software package [23]. A trial model for the structure was obtained from the phase sets generated by the SOLVER multistation software of NRCVAX. All non-hydrogen atoms were placed with a combination of difference Fourier and

Table 1. Crystallographic data for $[Zn(L)Cl][ClO_4](1)$

| | |
|--|----------------------------|
| Molecular formula | $ZnC_{12}H_{28}N_4O_4Cl_2$ |
| Formula weight | 428.66 |
| Crystal system | Orthorhombic |
| Space group | $P2_12_12_1$ |
| a (\AA) | 9.839(2) |
| b (\AA) | 9.953(2) |
| c (\AA) | 18.745(5) |
| V (\AA^3) | 1835.7(7) |
| Z | 4 |
| $F(000)$ | 898.37 |
| D_c ($Mg\ m^{-3}$) | 1.551 |
| Diffractometer | Enraf-Nonius CAD-4 |
| $\lambda/(Mo-K_\alpha)$ (\AA) | 0.71069 |
| $\mu(Mo-K_\alpha)$ (mm^{-1}) | 1.68 |
| Scan method | $\omega-2\theta$ |
| Scan width | $0.8 + 0.34 \tan \theta$ |
| h,k,l range | $0-11, 0-11, 0-22$ |
| 2θ range ($^\circ$) | $22.70-27.91$ |
| No. of unique reflections | 1766 |
| No. of observed reflections | 1372 |
| $[F_0 \geq 3\sigma F_0]$ | |
| R^a | 0.046 |
| R_w^b | 0.054 |
| GoF ^c | 0.88 |

^a $R = \Sigma(F_0 - F_c)/\Sigma(F_0)$.

^b $R_w = [\Sigma w(F_0 - F_c)^2/\Sigma(wF_0^2)]^{1/2}$.

^c $GoF = [\Sigma w(F_0 - F_c)^2/(\text{no. of rflns} - \text{no. params})]^{1/2}$.

least squares calculations. Hydrogen atoms in methyl groups were located from difference Fourier maps, other hydrogen atoms were placed in calculated positions. Anisotropic thermal parameters were used for all non-hydrogen atoms and isotropic thermal parameters were used with the hydrogen atoms. Hydrogen atom positions were fixed during the least squares process. Selected bond distances and angles for **1** are listed in Table 2. Full crystallographic details, atomic coordinates, interatomic distance and angles, hydrogen atom coordinates and anisotropic displacement parameters for **1** have been deposited with the editor as supplementary material. Structure factor tables may be obtained directly from the author.

RESULTS AND DISCUSSION

Crystal structure of [Zn(L)Cl][ClO₄](1)

The related macrocyclic tetraamine and their derivatives were earlier reported to form five- and six-coordinate zinc complexes with water [9–11] and thiocyanate [12] ligands. The crystal structure of the

complex **1** consists of a [Zn(L)Cl]⁺ cation and a perchlorate anion. A perspective drawing of **1** is shown in Fig. 1. The zinc atom is five-coordinate, distorted square pyramidal geometry with bonds to the four secondary amine nitrogen atoms of macrocycle and to the chlorine atom. The basal plane is slightly distorted [deviations N(1) 0.019(14), N(2) –0.018(14), N(3) 0.019(14) and N(4) –0.020(15) Å from the least-squares plane through these basal donor atoms] with zinc atom displaced 0.453(6) Å toward the apical chloride. The Zn–Cl(1) linkage is bent slightly off the perpendicular to the ZnN₄ plane by 11–14°. The average bond distance of 2.121(9) Å, between zinc and secondary nitrogens, which is comparable to that found in [Zn(DTAD)(NCS)][NCS] [12], indicates the distorted square pyramidal geometry. The Zn–Cl(1) bond distance in this complex is 2.275(3) Å, which is similar to that observed for a five-coordinated geometry (2.257 Å) [24]. The nitrogen atoms of macrocycle form two hydrogen bonds involving the perchlorate oxygens [N(2)⋯O(4), 3.16(2) Å and N(4)⋯O(2)ⁱ, 3.27(1) Å]. The N–Zn–N angles of the six-membered chelate rings of **1** are larger than those of the five-membered chelate rings. The methyl

Table 2. Bond lengths (Å) and angles(°) for [Zn(L)Cl][ClO₄](1)

| | | | |
|----------------|-----------|-------------------|-----------|
| Zn—Cl(1) | 2.275(3) | C(1)—C(2) | 1.510(20) |
| Zn—N(1) | 2.078(9) | C(3)—C(4) | 1.503(22) |
| Zn—N(2) | 2.159(10) | C(4)—C(5) | 1.534(18) |
| Zn—N(3) | 2.086(8) | C(5)—C(6) | 1.527(18) |
| Zn—N(4) | 2.161(8) | C(7)—C(8) | 1.501(20) |
| N(1)—C(2) | 1.462(17) | C(9)—C(10) | 1.491(19) |
| N(1)—C(3) | 1.464(18) | C(10)—C(11) | 1.500(18) |
| N(2)—C(5) | 1.466(15) | C(11)—C(12) | 1.537(19) |
| N(2)—C(7) | 1.466(15) | Cl(2)—O(1) | 1.402(11) |
| N(3)—C(8) | 1.486(17) | Cl(2)—O(2) | 1.328(11) |
| N(3)—C(9) | 1.458(17) | Cl(2)—O(3) | 1.354(16) |
| N(4)—C(1) | 1.476(16) | Cl(2)—O(4) | 1.336(15) |
| N(4)—C(11) | 1.480(16) | | |
| Cl(1)—Zn—N(1) | 104.1(3) | C(1)—N(4)—C(11) | 113.6(9) |
| Cl(1)—Zn—N(2) | 100.7(3) | N(4)—C(1)—C(2) | 110.1(11) |
| Cl(1)—Zn—N(3) | 102.1(3) | N(1)—C(2)—C(1) | 109.3(10) |
| Cl(1)—Zn—N(4) | 102.5(2) | N(1)—C(3)—C(4) | 113.6(10) |
| N(1)—Zn—N(2) | 89.0(4) | C(3)—C(4)—C(5) | 117.8(10) |
| N(1)—Zn—N(3) | 153.7(4) | N(2)—C(5)—C(4) | 109.8(10) |
| N(1)—Zn—N(4) | 82.5(4) | N(2)—C(5)—C(6) | 112.8(10) |
| N(2)—Zn—N(3) | 83.4(4) | C(4)—C(5)—C(6) | 111.7(11) |
| N(2)—Zn—N(4) | 156.6(3) | N(2)—C(7)—C(8) | 109.4(11) |
| N(3)—Zn—N(4) | 94.7(4) | N(3)—C(8)—C(7) | 110.3(10) |
| Zn—N(1)—C(2) | 106.7(7) | N(3)—C(9)—C(10) | 113.0(10) |
| Zn—N(1)—C(3) | 113.3(8) | C(9)—C(10)—C(11) | 116.7(10) |
| C(2)—N(1)—C(3) | 114.0(10) | N(4)—C(11)—C(10) | 112.1(11) |
| Zn—N(2)—C(5) | 112.6(7) | N(4)—C(11)—C(12) | 111.4(10) |
| Zn—N(2)—C(7) | 102.9(7) | C(10)—C(11)—C(12) | 111.9(11) |
| C(5)—N(2)—C(7) | 116.7(10) | O(1)—Cl(2)—O(2) | 110.7(8) |
| Zn—N(3)—C(8) | 108.3(7) | O(1)—Cl(2)—O(3) | 108.0(10) |
| Zn—N(3)—C(9) | 119.1(8) | O(1)—Cl(2)—O(4) | 109.8(9) |
| C(8)—N(3)—C(9) | 113.6(9) | O(2)—Cl(2)—O(3) | 110.8(11) |
| Zn—N(4)—C(1) | 107.5(8) | O(2)—Cl(2)—O(4) | 107.0(11) |
| Zn—N(4)—C(11) | 119.3(8) | O(3)—Cl(2)—O(4) | 110.7(16) |

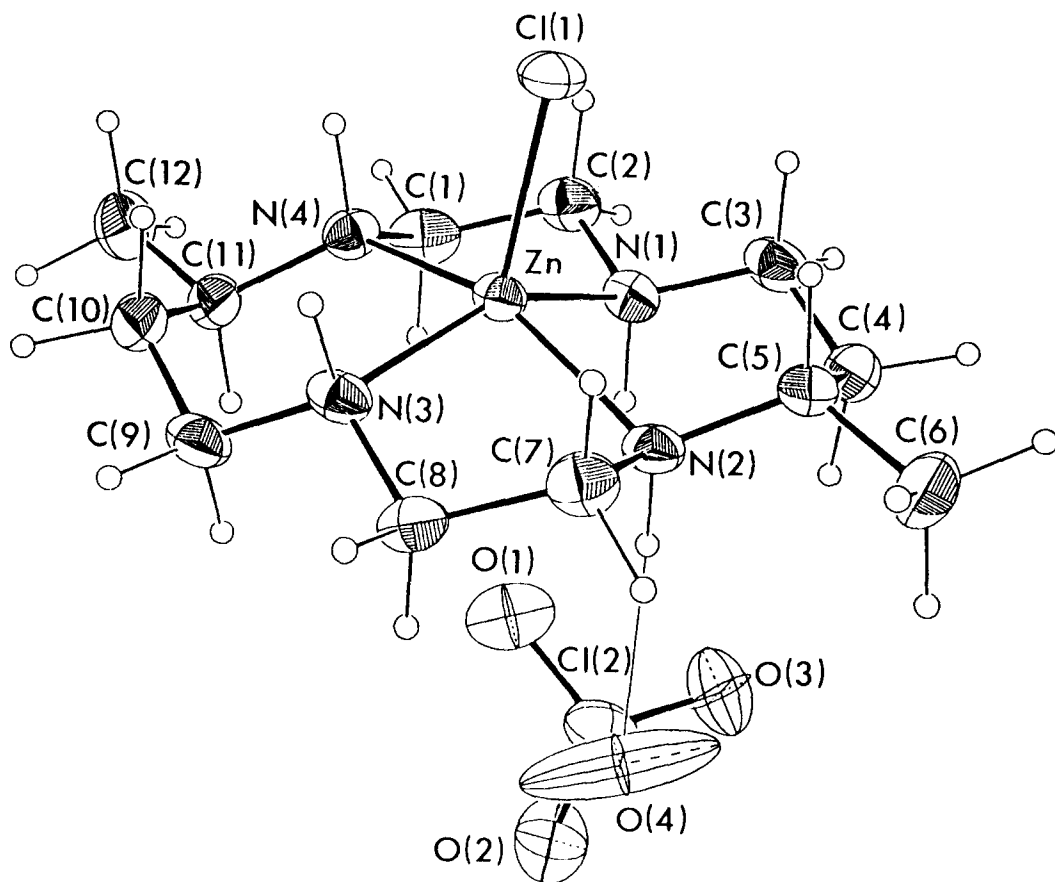


Fig. 1. ORTEP drawing of $[\text{Zn}(\text{L})\text{Cl}][\text{ClO}_4]\cdot(1)$ showing the atomic labelling scheme.

group on a six-membered chelate ring is anti with respect to the N_4 plane. As in the solid state structure of $[\text{Zn}(\text{L})][\text{ClO}_4]_2$ [20], $[\text{Zn}(\text{DTAD})(\text{H}_2\text{O})_2]\text{Cl}_2$ [11] and $[\text{Zn}(\text{DTAD})\text{NCS}][\text{NCS}]$ [12], **1** also adopts a thermodynamically most stable *trans*-III conformation in the solid state.

Formation kinetics

The formation reaction of $\text{M}(\text{L})^{2-}$ complexes was studied under pseudo-first-order conditions in a lightly buffered medium with M^{2+} in large excess. The observed rate constants follow eq. (1),

$$\frac{d[\text{M}(\text{L})^{2-}]/dt = k_{\text{obs}}[\text{L}]_{\text{T}}, \quad (1)$$

where $[\text{L}]_{\text{T}}$ is the concentration of the various protonated forms of the ligand and k_{obs} is a pseudo-first-order rate constant. At a given pH 4.58–5.50, the k_{obs} values increased with increasing $[\text{M}^{2+}]$ and the plot of

k_{obs} vs $[\text{M}^{2+}]$ gave a saturation curve. This behaviour can be rationalized in terms of an intermediate complex formation in the equilibrium step, followed by its rearrangement in the rate-determining step. The relationship between k_{obs} and $[\text{M}^{2+}]$ can be described [25] by

$$k_{\text{obs}} = \frac{k_1 K [\text{M}^{2+}]}{1 + K [\text{M}^{2+}]}, \quad (2)$$

where K is the equilibrium constant characterizing the formation of an intermediate and k_1 is the rate constant for rearrangement of the intermediate to the final product. Plots of $1/k_{\text{obs}}$ against $1/[\text{M}^{2+}]$ lead to straight line as shown in Fig. 2. The values of k_1 , K and the second-order rate constant $k_2 = k_1 K$ were deduced from eq. (2) and summarized in Table 3. The resolved values of K were independent of pH while the values of k_1 were pH dependent as shown in Table 3. The protonated forms of **L** could contribute to the complexation of M^{2+} ions between pH 4.58 and 5.50. The concentrations of protonated ligands were computed with the use of ligand protonation constants[†]. In this pH range, H_2L^{2-} is the major species (99.34–99.92%) while HL^{3-} is very low (1.0×10^{-4} –

[†]Protonation constants ($\log K_i$) in 0.10 M NaClO_4 and at $25.0 \pm 0.1^\circ\text{C}$ are 11.68, 10.36, 2.28 and 1.96, which were calculated by fitting the potentiometric data to the PKAS program [26].

Table 3. Rate data for the metal complexation with L at $25.0 \pm 0.1^\circ\text{C}$, $I = 0.10 \text{ M}$ (NaClO_4) and $[\text{OAc}^-] = 1.0 \times 10^{-2} \text{ M}$

| Metal ions | pH | $k_1(\text{s}^{-1})$ | $K(\text{M}^{-1})$ | $k_2(\text{M}^{-1} \text{s}^{-1})$ |
|------------------|------|-----------------------|--------------------|------------------------------------|
| Zn^{2+} | 4.58 | 2.93 | 1.03×10^2 | 3.01×10^2 |
| | 4.78 | 3.60 | 1.05×10^2 | 3.79×10^2 |
| | 4.94 | 4.42 | 1.05×10^2 | 4.64×10^2 |
| | 5.18 | 6.38 | 1.08×10^2 | 6.90×10^2 |
| | 5.32 | 8.29 | 1.06×10^2 | 8.80×10^2 |
| | 5.50 | 11.5 | 1.10×10^2 | 12.6×10^2 |
| Cu^{2+} | 4.58 | 1.33×10^{-2} | 1.41×10^2 | 1.88 |
| | 4.79 | 1.81×10^{-2} | 1.40×10^2 | 2.52 |
| | 4.96 | 2.30×10^{-2} | 1.38×10^2 | 3.18 |
| | 5.20 | 3.25×10^{-2} | 1.42×10^2 | 4.60 |
| | 5.30 | 3.94×10^{-2} | 1.42×10^2 | 5.59 |
| | 5.50 | 5.63×10^{-2} | 1.43×10^2 | 8.05 |

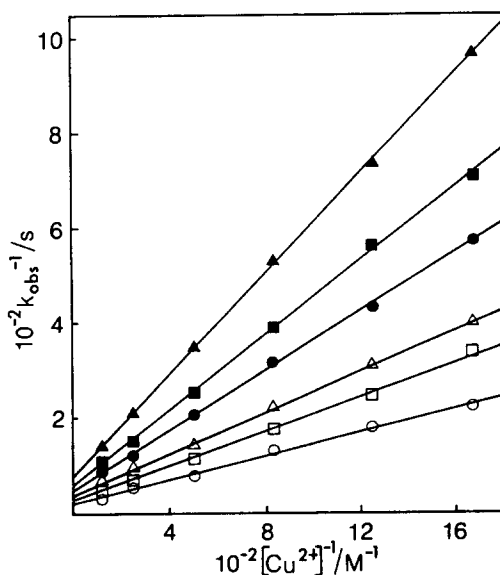


Fig. 2. Plots of k_{obs}^{-1} vs $[\text{Cu}^{2+}]^{-1}$ for the formation kinetics of $\text{Cu}(\text{L})^{2-}$ at different pH values. $[\text{OAc}^-] = 0.01 \text{ M}$, $T = 25.0 \pm 0.1^\circ\text{C}$, $I = 0.10 \text{ M}$ (NaClO_4); pH = 4.58(▲), 4.79(■), 4.96(●), 5.20(△), 5.30(○), 5.50(□).

$1.1 \times 10^{-3}\%$). The overall stability constant of the intermediate (MH_2L^{2-}) can be determined by the value of K at given pH, the ligand protonation constant and with the use of eq. (3).

$$K_{\text{MH}_2\text{L}^{2-}} = K(1 + K_3[\text{H}^+] + K_3K_4[\text{H}^+]^2). \quad (3)$$

The calculated values of $\log K_{\text{MH}_2\text{L}^{2-}}$ are summarized

†The stability constants in 0.10 M NaClO_4 and at $25.0 \pm 0.1^\circ\text{C}$ were obtained from the potentiometric data and the ligand protonation constants with the aid of the BEST program [26].

in Table 4. The stability constant for the intermediate of $\text{Cu}(\text{L})^{2-}$ complex is somewhat higher than that of $\text{Zn}(\text{L})^{2-}$. This fact may be attributed to the thermodynamic stability ($\log \beta_{\text{Cu}(\text{L})^{2-}} = 27.81$ vs $\log \beta_{\text{Zn}(\text{L})^{2-}} = 16.06$)†.

The second-order rate constant k_{HnL} also represents $(k_1K)_{\text{HnL}}$ from the kinetic data. If one species is markedly more reactive than all the other, the second-order rate constant could be obtained from the following expression [21]

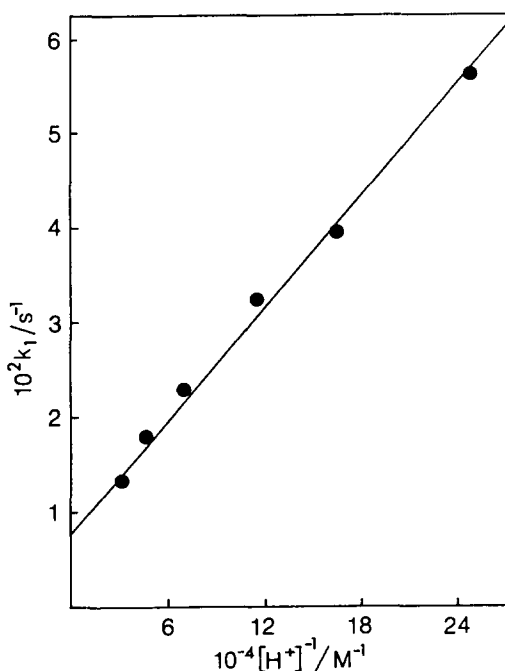
$$k_2 = k_{\text{HnL}}(1 + K_{\text{H}(\text{n}+1)\text{L}}[\text{H}^+])^{-1}, \quad (4)$$

where $K_{\text{H}(\text{n}+1)\text{L}}$ is the protonation constant of ligand. From the plots of k_2 against $(1 + K_{\text{H}(\text{n}+1)\text{L}}[\text{H}^+])^{-1}$, the second-order rate constants for the HL^{3-} and H_2L^{2-} species obtained are collected in Table 4 along with the literature values [14,15]. Despite of their very low concentration in the pH range observed, monoprotonated form HL^{3-} species appears to be kinetically much more reactive than diprotonated species H_2L^{2-} even though the latter is the major component in solution. Kodama and Kimura [14,15] demonstrated that the monoprotonated form HL^{3-} was 4–8 orders of magnitude more reactive than the diprotonated form H_2L^{2-} in the case of the reaction of Zn^{2+} and Cu^{2+} with cyclam. The low reactivity of H_2L^{2-} may be ascribed to the two protons being maintained near the coordination site, increasing electrostatic repulsion.

The rate constant k_1 for rearrangement of the intermediate increased with increasing pH as shown in Table 3. This observation is consistent with previously reported works [18,27,28]. The values of k_1 were found to be inversely proportion to $[\text{H}^+]$ as shown in Fig. 3. This relationship indicates that the rearrangement of the intermediate complex into the final chelate product is catalysed by the OH^- ion. An expression consistent with this functional dependence is given by eq. (5) [27,28]

Table 4. Stability constants ($\log K_{\text{MH}_2\text{L}^{2-}}$), second-order rate constants ($k_{\text{H}_2\text{L}}$) and base-catalyzed rate constant (k_{OH}) of the intermediate complexes at $25.0 \pm 0.1^\circ\text{C}$ and $I = 0.10 \text{ M}$ (NaClO_4)

| Complexes | $\log K_{\text{MH}_2\text{L}^{2-}}$ | $k_{\text{H}_2\text{L}^{2-}} (\text{M}^{-1} \text{s}^{-1})$ | $k_{\text{HL}^-} (\text{M}^{-1} \text{s}^{-1})$ | $k_{\text{OH}} (\text{M}^{-1} \text{s}^{-1})$ |
|---------------------|-------------------------------------|---|---|---|
| Zn(L) $^{2-}$ | 2.03 ± 0.02 | $(1.43 \pm 0.46) \times 10^5$ | $(1.01 \pm 0.02) \times 10^8$ | $(2.40 \pm 0.04) \times 10^9$ |
| Zn(cyclam) $^{2-a}$ | ^b | 1.0 | 7.5×10^4 | ^b |
| Cu(L) $^{2-}$ | 2.15 ± 0.01 | $(9.10 \pm 2.81) \times 10^3$ | $(6.44 \pm 0.08) \times 10^5$ | $(1.17 \pm 0.07) \times 10^7$ |
| Cu(cyclam) $^{2-a}$ | ^b | 0.08 | 8.0×10^6 | ^b |

^a References 14 and 15.^b Not observed.Fig. 3. Plots of k_1 vs $[\text{H}^+]^{-1}$ for the formation kinetics of $\text{Cu}(\text{L})^{2-}$ at $25.0 \pm 0.1^\circ\text{C}$ and $I = 0.10 \text{ M}$ (NaClO_4).

$$k_1 = (k_{\text{H}_2\text{O}} + k_{\text{OH}} K_{\text{W}} / [\text{H}^+]), \quad (5)$$

where $k_{\text{H}_2\text{O}}$ and k_{OH} are water and hydroxide-catalysed rate constant for rearrangement of the intermediate. The value of k_{OH} calculated the slope of the straight line in Fig. 3 and eq. (5) ($\log K_{\text{W}} = 13.78$) is listed in Table 4. A significant contribution from the base form of the buffer is not expected, since the concentration of buffer used in the present work is low. The k_{OH} value of $\text{Cu}(\text{L})^{2-}$ is about two orders of magnitude smaller than that of $\text{Zn}(\text{L})^{2-}$. This is presumably due to increase of thermodynamic stability by the difference in ionic size which is mentioned already.

Acknowledgement—This work was supported by the Research Fund of Mokwon University, 1996.

REFERENCES

1. K. D. Karlin and Z. Tyeklar, *Bioinorganic Chemistry of Copper*. Chapman & Hall, New York, London (1993).
2. I. Bertini and C. Luchinat, in *Bioinorganic Chemistry* (Edited by I. Bertini, H. B. Gray, S. J. Lippard and J. Valentine). University Science Books, Mill Valley, CA (1994).
3. L. Fabbrizzi, *Comments Inorg. Chem.* 1985, **4**, 33.
4. C. M. Che, K. Y. Wong and C. K. Poon, *Inorg. Chem.* 1986, **25**, 1809.
5. E. Kimura, Y. Kotake, T. Koike, M. Shionoya and M. Shiro, *Inorg. Chem.* 1990, **29**, 4991.
6. M. Shionoya, E. Kimura and Y. Iitaka, *J. Am. Chem. Soc.* 1990, **112**, 9237.
7. E. Fujita, J. Haff, R. Sanzenbacher and H. Elias, *Inorg. Chem.* 1994, **33**, 4627.
8. K. Y. Choi, J. C. Kim, W. P. Jensen, I. H. Suh and S. S. Choi, *Acta Cryst., Sect. C* 1996, **52**, 2166.
9. E. Kimura, T. Shiota, T. Koike, M. Shiro and M. Kodama, *J. Am. Chem. Soc.* 1990, **112**, 5805.
10. X. Zhang and R. van Eldik, *Inorg. Chem.* 1995, **34**, 5606.
11. K. Y. Choi, I. H. Suh and J. C. Kim, *Polyhedron*, in press.
12. K. Y. Choi and I. H. Suh, *Polyhedron*, in press.
13. K. Y. Choi, M. R. Oh and I. H. Suh, *Chem. Lett.*, in press.
14. M. Kodama and E. Kimura, *J. Chem. Soc., Dalton Trans.* 1977, 1473.
15. M. Kodama and E. Kimura, *J. Chem. Soc., Dalton Trans.* 1977, 2269.
16. K. Y. Choi and C. P. Hong, *Bull. Kor. Chem. Soc.* 1994, **15**, 293.
17. K. Y. Choi, D. W. Kim and C. P. Hong, *Polyhedron* 1995, **14**, 1299.
18. K. Y. Choi, S. H. Kang, D. W. Kim, Y. S. Chung, C. S. Kim, J. J. Oh, C. P. Hong and Y. I. Lee, *Supramol. Chem.* 1996, **7**, 27.
19. K. Y. Choi, D. W. Kim, C. S. Kim, C. P. Hong, H. Ryu and Y. I. Lee, *Talanta*, in press.
20. R. W. Hay and P. P. Dharam, *J. Chem. Soc., Dalton Trans.* 1975, 1956.
21. S. P. Kasprzyk and R. G. Wilkins, *Inorg. Chem.* 1982, **21**, 3349.
22. K. Y. Choi and G. R. Choppin, *J. Coord. Chem.* 1991, **24**, 19.

23. E. J. Gabe, Y. L. Page, J. P. Charland, F. L. Lee and P. S. White, *J. Appl. Cryst.* 1989, **22**, 384.
24. A. G. Orpen, L. Brammer, F. H. Allen, O. Kennard, D. G. Watson and R. Taylor, *J. Chem. Soc., Dalton. Trans.* 1989, S1.
25. R. G. Wilkins, *The Study of Kinetics and Mechanism of Reaction of Transition Metal Complexes*, p. 26. Allyn and Bacon, Boston, MA (1974).
26. A. E. Martell and R. J. Motekaitis, *The Determination and Use of Stability Constants*. VCH, New York (1992).
27. K. Kumar and M. F. Tweedle, *Inorg. Chem.* 1993, **32**, 4193.
28. K. Kumar, T. Jin, X. Wang, J. F. Desreux and M. F. Tweedle, *Inorg. Chem.* 1994, **33**, 3823.